VTT Technical Research Centre of Finland

On the enhancement of coupling potential flow models to RANS solvers for the prediction of propeller effective wakes

Sanchez Caja, Antonio; Martio, Jussi; Saisto, Ilkka; Siikonen, T

Published in:
Journal of Marine Science and Technology

DOI:
10.1007/s00773-014-0255-4

Published: 01/01/2015

Document Version
Peer reviewed version

Journal of Marine Science and Technology, February 2014, DOI 10.1007/s00773-014-0255-4

On the Enhancement of Coupling Potential Flow Models to RANS solvers for the Prediction of Propeller Effective Wakes

A. Sánchez-Caja[1], J. Martio[1], I. Saisto[1] & T. Siikonen[2]
([1]VTT Technical Research Center of Finland)
([2]Aalto University)

ABSTRACT

The calculation of the effective wake within the CFD context is usually made by combining a potential flow method for modeling the propeller forces with a RANS equation solver for simulating the viscous flow around the hull and possible appendages. The different assumptions and/or simplifications made in the potential flow model relative to the viscous flow solver may result in significant errors in the prediction of the effective wake particularly for high loadings. This is especially troublesome for ships with full forms where large differences are expected between the nominal and effective wake, and for special propulsion applications such as contra-rotating units. Such errors are responsible within the hydrodynamic design problem for an unadjusted prediction of the propeller pitch, and within the hydrodynamic analysis problem for a deficient prediction of self-propulsion point.

This paper presents an approach based on correction factors which converts propeller induced velocities approximately estimated via potential flow theory into viscous induced velocities on the basis of a viscous flow RANS analysis. The correction factors are calculated for one reference advance number and work accurately in a neighboring region where the propeller loading may change about +/- 50 percent. This procedure allows controlling one of the errors present in the calculation of effective wakes, namely the error derived from coupling a potential flow method for the representation of the propeller with a RANS solver. Consequently, it permits calculating the effective wake more precisely. The approach is illustrated for a simple case in which the potential flow model representing the propeller is an actuator disk.

1. INTRODUCTION

Generally, the success of a propeller design depends on the accurate estimation of the effective wake. This is especially true for full-form ships where large differences are expected between the nominal and the effective wakes. In addition, within the CFD context, the accurate estimation of the ship self-propulsion point depends also on the use of the correct effective wake.

Typically, errors of 2-5 percent in the estimation of the effective wake could lead to errors of 5-14 percent in the estimation of force coefficients for usual propeller loadings. Furthermore, an exact prediction of not only the axial but also the tangential effective wake may be critical in some particular applications such as CRP units. For contra-rotating propellers the effective wake at the plane of each propeller depends not only on the shape of hull form but also on the effect of the other propeller and possible surrounding appendages. This effect is especially relevant when the axial and tangential wakes are estimated at the location of the aft propeller, which is subject to the slipstream of the fore one.

Within the CFD framework, the estimation of the effective wake at the propeller plane is usually made by combining a RANS solver for modeling the turbulent flow around the ship hull with a potential flow method for simulating the propeller action. Typically, the propeller-induced velocities resulting from the potential flow solver are first calculated by an actuator disk (AD) model and then subtracted from the total velocities obtained in the RANS computation. In this way the effective wake is obtained.

It is well known that the axial and tangential propeller-induced velocities behave in different ways over the propeller plane. The circumferentially averaged axial velocities increase in a uniform way as the flow go past the actuator disk whereas the tangential velocities experience a sudden jump at the disk. Consequently, the large gradients in the direction of the propeller axis for the tangential flow make it difficult to define the tangential induced velocities at the propeller plane. These velocities need special

treatment for the determination of an accurate effective wake in CRP units.

Additionally, potential flow methods for propeller design include simplifications concerning the shape of the propeller wake (e.g. lightly versus moderately loaded wake models in propeller lifting line or actuator disk theory), the inclusion or not of the hub effect, etc. These simplifications would affect the accuracy of the effective wake predictions when such methods are coupled to RANS solvers. In other words, potential flow theory for a given propeller load yields induced velocities that are not exactly equal to those derived from a RANS solver with equivalent body forces for the same propeller load. It would then be desirable that such methods when coupled to viscous RANS solvers do not introduce errors in the estimation of effective wakes and consequently, of propeller loads. In the literature, quantification of such errors for coupling a panel method with a RANS solver is shown for example by Rijpkema et al. (2013) and Kinnas et al. (2013).

This paper presents ways to enhance current methods for estimating effective wakes with an accuracy which is not much affected by the simplifications introduced in the basic potential flow propeller model. For this purpose a numerical approach has been developed which relies on correction factors. Such factors are calculated only for one advance number and they succeed to yield accurate estimations of the effective wake when applied to other advance numbers located in a wide region in the vicinity of it.

From the standpoint of hydrodynamic *design* the approach will provide the propeller designer with an accurate estimation of the inflow. From the standpoint of hydrodynamic *analysis* the approach is expected to improve the estimation of the ship self-propulsion point using RANS methods. As the knowledge of the nominal wake at the propeller plane is not a sufficient input for determining the effective wake, the approach presented here is intended mainly for computational domains including all surrounding bodies which may affect the effective wake. The paper deals also with the prediction of tangential effective wakes, which is important for the design of CRP propellers.

An off-design lifting line model is used for the demonstration of the method and an application to a CRP pod propulsion unit called RudderPod will be made in order to illustrate the magnitude of the coupling errors in a practical case. The RudderPod is a non-rotatable podded propulsor where the strut is enlarged with a rudder for steering. It works as the aft-propeller of a CRP unit located behind the main propeller. Due to the fact that the pod is non-rotatable manufacturing is cheap.

2. LITERATURE REVIEW

Effective Wake

Notionally, the flow at the location of the propeller consist of three components: the flow as altered by the ship hull in the absence of the propeller (*nominal wake*), the propeller induced velocities (*induced wake*) and the interaction between the two preceding flows (*interaction wake*). The interaction wake is a result of changes not only in boundary layer thickness (or more generally in spatial distribution of vorticity) but also in factors like wave patterns, which may be altered by the propeller suction and may in turn modify the velocity field at the propeller plane, etc. Then, the *effective* wake is defined as the sum of the nominal wake and the interaction wake. At this point it should be noted that the effective wake cannot be measured directly in experiments, since only the total velocities are directly measurable in the experimental tests.

The simulation of the effective wake by RANS methods has been treated in the literature mainly by actuator disk models. Generally, most of the actuator disk models coupled to viscous solvers rely on body forces constant in time (Lobatchev et al, 2001; Hoeskstra, 2006). Some others modify the strength of the body forces in an interactive way as the computation proceeds on the basis of the updated incoming flow (Zhang et al., 1991; Stern et al., 1994; Kerwin et al., 1994; Choi et al., 2001; Sánchez-Caja & Pylkkänen 2007; Kinnas et al. 2009, 2012). The latter approach is used for finding the effective wake and self-propulsion point of a ship for a given propeller geometry and rate of revolutions. This approach is followed here.

Propeller-Pod Housing Interaction

The interaction between propeller and pod housing analyzed in the application part of this paper is similar to that between propeller and rudders. Such interaction has been studied numerically in the literature by several researchers. Suzuki, et al. (1993) performed viscous flow computations of propeller-rudder interaction using a viscous flow code coupled with a body force distribution which represented the propeller. He studied also the effect of the rudder on powering performance coefficients. Coupled potential methods for the analysis of propeller-rudder interaction via circumferential averaged flow are also found in Li (1994, 1995), Lee et al. (2003), Greco and Salvatore (2004), Kinnas et al. (2007). Han and Kai-Jia (2008) studied hull/propeller/rudder interaction by coupling a RANS solver to either a vortex lattice lifting surface or a lifting line propeller model via body forces. Sánchez-Caja et al. (2008) studied the propeller rudder interaction with a full RANS representation of

propeller and rudder. The impact of the mixing-plane, quasi-steady and unsteady approaches on the results was illustrated in Sánchez-Caja et al. (2009).

Concerning podded propulsors, the unsteady interaction of pod propulsor with a fully representation of the propeller and housing geometries was simulated using a RANS viscous solver in Sanchez-Caja et al. (1999) and scale effects were analyzed in Sanchez-Caja et al. (2003). Hsin et al. (2002) used a coupled viscous/potential flow method. Ohashi and Hino (2004) analyzed the viscous flow around a ship hull propelled by a CRP unit which was modeled using body forces in unstructured grids. Kinnas et al. (2009) used a vortex lattice lifting surface method combined with two different RANS solvers for the estimation of the effective wake on a podded propulsor.

3. NUMERICAL APPROACH

RANS Solver

The flow simulation is made with RANS solver FINFLO. A description of the numerical method including discretization of the governing equations, solution algorithm, etc. can be found in Sanchez-Caja et al. (1999). The solution of the RANS equations is obtained by the pseudo-compressibility method. The momentum equations can be written in the following form

$$\rho\frac{D\vec{V}}{Dt} + \nabla p - \mu\nabla^2\vec{V} = \rho\vec{g} + \vec{F}_{AD}$$

where $\vec{V}$ is the velocity vector, ρ is the density, μ is the dynamic viscosity, $\vec{g}$ the acceleration of gravity and $\vec{F}_{AD}$ are the forces generated by the actuator disk. The equation can be expressed in terms of a vector U of conservative variables $(\rho, \rho u, \rho v, \rho w, \rho k, \rho\varepsilon)^T$, where u, v and w are the absolute velocity components; k is the turbulent kinetic energy and ε is the dissipation of k. For the steady-state analysis with a full representation of the propeller (i.e. without actuator disk simplifications), the equations are solved in a co-ordinate system that rotates around the x-axis with an angular velocity Ω. In that case, the RHS of the momentum equation has the additional component $(0, 0, \rho\Omega w, -\rho\Omega v, 0, 0)$. For time-accurate simulations, the source terms for the turbulence equations are retained, but there are no source terms in the momentum equations except gravitation and the force generated by the actuator disk.

In the pseudo-compressibility approach the continuity equation is replaced by

$$\frac{1}{\beta^2}\frac{\partial p}{\partial t} + \nabla\cdot\vec{V} = 0$$

being β the pseudo-compressibility factor.

FINFLO solves the RANS equations by a finite volume method. The implicit solution is based on approximately factorized time-integration with local time-stepping. In the present incompressible case the code uses an upwind-biased approximation for convective fluxes, while either Roe's flux-difference splitting or Van Leer's flux-vector splitting is applied for compressible flows. In the incompressible case, a Rhie and Chow type method has been implemented in the code in the simplified form presented by Johansson et al. (1995). The pressure is central-differenced and a damping term is added via a convective velocity. A multigrid method is used for the acceleration of convergence. Solutions on the coarse grid levels are used as starting point for the calculation in order to accelerate convergence. A viscous solution is extended to the wall and Chien's k-epsilon turbulence model was used in the present simulations.

Potential Flow Model for the Propeller

The potential flow method used for modeling the propeller action is a vortex-lattice lifting line model working in off-design mode. The model takes into account the actual geometry of the blades (pitch and flow angle of attack, etc.) and therefore, the circulation developed on the lifting lines is dependent on such blade parameters as well as on the variation of inflow velocities. Additionally the model includes lifting surface correction factors for camber, ideal angle of attack and thickness. Even though the model is simple, our main goal is to demonstrate a correction factor procedure, which could be extended to more sophisticated potential flow methods, like lifting surface or panel methods. Other assumptions that the lifting-line theory adopts are those presented in Kerwin et al., (1986):

- The propeller blades are represented by straight, radial lifting lines. The lifting lines are divided into a discrete number of straight-line segments. The vortex strength is constant within each segment but can vary from segment to segment. In order to treat adequately the square-root singularity that appears at the tips of the lifting lines, the dimensions of the segments are either constant with one quarter inset at the tips or distributed according to the so-called cosine law.

- The propeller blades have equal angular spacing and identical loading. Besides, the loading is considered time-independent since the onset flow to the propeller is circumferentially averaged in lifting-line calculations.

- The wake geometry is assumed to be purely helical, with a pitch at each radius determined by the induced flow at the lifting line (moderately loaded theory). The wake consists of a discrete number of free vortices that are shed from the edges of the lifting-line

segments. Their strength according to Kelvin's theorem of conservation of vorticity is given by the difference of strengths between the two adjacent segments.

The method includes an optional pitch-reduction feature for the tip vortices shed from the blades where the pitch of the tip vortices is calculated as an average between the flow inside and outside the slipstream of the propeller.

Coupling RANS and Potential Flow Solvers

A potential-flow lifting-line (LL) method is interactively combined with a viscous RANS solver to predict the effective wake at the propeller location. Propeller forces obtained from the potential flow solver are expressed in terms of axisymmetric body forces and introduced as input to the viscous solver. In turn, an effective wake field is derived from the RANS solver by subtracting the axisymmetric component of the propeller induced velocities from the total velocities in the bulk flow. The effective wake thus obtained will be the input to the LL code for the next iteration. The lifting line calculation is integrated into the viscous solver so that it is made only once within each iteration. The very short CPU time required by the lifting line subroutine does not increase noticeably the overall computational time of the RANS solver.

The radial distribution of loading on the propeller blade resulting from the lifting line calculation is uniformly spread at each radial station in the circumferential direction and expressed in terms of axial and tangential forces per unit volume. The body forces generating thrust (f_T) and torque (f_Q) can be written as

$$f_T = \frac{\rho Z}{\upsilon}\left[\sum_{m=1}^{M}\left(V_{T,m}+\omega r_m+U^*_{T,m}\right)\Gamma_m\Delta r_m - \sum_{m=1}^{M}\frac{1}{2}V^2_{E,m}c_m C_{D,m}\sin\beta_{I,m}\Delta r_m\right] \quad (1)$$

$$f_Q = \frac{\rho Z}{\upsilon}\left[\sum_{m=1}^{M}\left(V_{A,m}+U^*_{A,m}\right)\Gamma_m r_m\Delta r_m - \sum_{m=1}^{M}\frac{1}{2}V^2_{E,m}c_m C_{D,m}\cos\beta_{I,m} r\Delta r_m\right] \quad (2)$$

where at panel m, r_m is the radius, $V_{A,m}$ is the axial inflow, $V_{E,m}$ the effective total velocity, $U^*_{A,m}$ and $U^*_{T,m}$ the propeller-induced axial and tangential velocities at the lifting line respectively, Γ_m the circulation, c_m the local chord, $C_{D,m}$ the drag coefficient, $\beta_{I,m}$ the induced angle of attack, Δr_m is the panel length, M is the number of panels on the LL, Z the number of blades, ρ is the water density and υ is the circumferential volume over which the forces are spread. The body forces are then transformed into Cartesian components.

In the present study the propeller suction is modeled as the suction of an equivalent actuator disk. Only a one-cell layer of body forces is used in the propeller axial direction, even though more layers could be used if needed. This would be the case for example when the potential flow method is a lifting surface or a panel method. When using one cell layer we are interested in the effective wake on the propeller plane, not on the actual location of the blades. The width of the layer will determine the sharpness of the actuator disk solution. The propeller rake can be easily introduced in the model by adapting the grid shape to the rake line. This approach allows calculating the effective wake directly from the velocity field at the propeller plane. The effective *axial* wake is extracted at this layer of cells (i.e. at the propeller plane) by subtracting the propeller induced velocities from the total velocities in the RANS computation. In order to avoid inaccuracies in the prediction of the effective *tangential* wake due to the large axial gradients in the tangential flow at the propeller plane a special treatment is made. The total velocities are taken from a layer 3-5 cells upstream of the propeller plane. The width of such cells can be made small so that the location of the control points is very close to the actual propeller plane. The advantage of this approach is clear, since upstream of the propeller plane the circumferentially-averaged self-induced tangential velocities are zero. The 3-5 cell layer choice guarantees the adequate sharpness of the solution.

In fact, we are reproducing in the RANS context an actuator disk solution which is characterized by having zero induced tangential velocities in front of the disk. The sharpness of the actuator disk solution can be controlled by the axial width of the cell layer, which in fact means that we can go as close to the propeller disk as we want. The convergence of the solution can be checked through Table IV, where the ratio of the cells for the coarse and fine grid is 2, and the results remain unaltered. The axial convection of the flow does not allow tangential velocities to spread upstream. Only a small departure from zero is present in 1-3 cell layers next to the disk due mainly to the differential scheme. In our particular case the tangential velocities are taken upstream the propeller plane at a distance less than 0.05 times the propeller diameter. This distance could be further reduced if needed. This approach avoids the problems mentioned in Rijpkema et al. (2013) about the selection of the extraction planes due to strong axial gradients in axial effective wakes for ship propellers in behind condition.

Correction Factors

The accuracy of the coupling technique in estimating the effective wake would depend on the ability of the off-design lifting-line method to reproduce the field of induced velocities generated by the body forces within the RANS solver. Usually, the velocities induced by the viscous solver are close but do not coincide with those estimated by the potential LL code. This introduces an error in the prediction of the effective wake, which in turn will result in design errors when estimating the propeller pitch. The differences will be more significant for large propeller loadings.

An easy way of estimating such wake errors is to apply the coupling methodology explained in the preceding section to calculate the effective wake due to a propeller alone (i.e. in the presence of no surrounding bodies) subject to a *uniform flow*. For this simple setup the solution is known: the axial effective wake is the uniform inflow, i.e.

$$\frac{V_{A,Bulk} - U_A^{exact}}{V_A} = 1 \qquad (3)$$

where $V_{A,Bulk}$ is the total axial velocity of the bulk flow in the RANS solver on the propeller plane, V_A is uniform inflow at the inlet of the domain and U_A^{exact} is the exact circumferentially-averaged propeller-induced axial velocity within the RANS solution.
However, the induced axial velocity predicted by the potential flow solver U_A will differ from the exact one and a correction to U_A can be expressed as follows,

$$\frac{\Delta U_A}{V_A} = 1 - \frac{V_{A,Bulk} - U_A}{V_A} \qquad (4)$$

where ΔU_A represents the correction term that should be applied so that the potential flow induced velocities U_A will be converted into 'viscous' flow induced velocities, U_A -ΔU_A.

The corrections can be calculated either inside or outside the iteration process in the RANS solver code. In the former case ("exact" approach), the corrections are calculated at the end of each iteration loop and introduced into the viscous solver for the next iteration. When convergence is reached, the final loading of the propeller will be that resulting from a potential flow calculation at the trial advance number, and the effective wake will be *exactly* the inflow V_A provided that the 'viscous' induced velocities of magnitude U_A - ΔU_A are used in the updating procedure.

In the latter case ("approximate" approach), a trial run for effective wake prediction is made with no corrections and from this calculation an *approximate* guess for the corrections may be derived. After reaching convergence equation (4) can be used to obtain from the induced velocities U_A an initial estimation of the corrections $\Delta U_A^{init.}$. Contrary to the former procedure, as these corrections were not implemented inside the iteration loop, the effective wake thus obtained will not be exactly the inflow V_A, but V_A-ΔU_A. Consequently, the propeller loading will differ somewhat from the exact one. The final estimation of the corrections for this loading will be made on the basis of the propeller induced axial velocities U_A. A proportionality can be established with this purpose: noting that $\Delta U_A^{init.}$ corresponds to induced velocities of magnitude U_A-ΔU_A^{final} (not U_A), and that $\Delta U_A^{final.}$ corresponds to U_A,

$$U_A \Delta U_A^{init} = (U_A - \Delta U_A^{final}) \Delta U_A^{final} \qquad (5)$$

Notice also that if ΔU_A is a zero of first order, the difference between ΔU_A^{init} and ΔU_A^{final} is a zero of second order.

$$\frac{\Delta U_A^{final}}{V_A} = \frac{1}{V_A}\left[\frac{U_A - \sqrt{U_A^2 - 4U_A \Delta U_A^{init}}}{2}\right] \qquad (6)$$

Once the corrections to the induced velocities are derived from one of the previous procedures, correction factors can be introduced. If V_{A0} represents the inflow at a reference advance number J_0 where the correction term is ΔU_{A0}, the correction term (ΔU_{A1}) at other advance number J_1 can be estimated (ΔU^*_{A1}) on the basis of the reference correction as follows,

$$\frac{\Delta U^*_{A1}}{V_{A1}} = \frac{\Delta U_{A0}}{V_{A0}}\left[\frac{U_{A1}/V_{A1}}{U_{A0}/V_{A0}}\right] \qquad (7)$$

This approach allows defining correction factors (F_A) that are independent of the advance number:

$$F_{A0} = \frac{U_{A0} - \Delta U_{A0}}{U_{A0}} = \frac{U_{A1} - \Delta U^*_{A1}}{U_{A1}} = F_{A1} \qquad (8)$$

These correction factors should work accurately in the neighborhood of the reference advance number and, therefore, need to be evaluated only once (for reference advance number). In practical applications the reference advance number can be chosen around that corresponding to the nominal wake fraction.

Analogously, a correction term can be defined for the tangential induced velocities. In this case the solution to the tangential effective wake is zero, so the equivalent expressions to equations (4), (7) and (8) are

$$\frac{\Delta U_T}{V_A} = 0 - \frac{V_{T,Bulk} - U_T}{V_A} \qquad (9)$$

$$\frac{\Delta U_{T1}^{*}}{V_{A1}} = \frac{\Delta U_{T0}}{V_{A0}}\left[\frac{U_{T1}/V_{A1}}{U_{T0}/V_{A0}}\right] \quad (10)$$

$$F_{T0} = \frac{U_{T0} - \Delta U_{T0}}{U_{T0}} = \frac{U_{T1} - \Delta U_{T1}}{U_{T1}} = F_{T1} \quad (11)$$

However, the correction for the effective tangential wake can be avoided provided that the cell layer used to evaluate the tangential wake is chosen 3-5 cells upstream from the propeller plane, where the body forces do not induce tangential velocities and the errors in tangential wake prediction would be negligible.

Equation (6) can be expressed in terms of correction factors as

$$\frac{\Delta U_A^{final}}{V_A} = \frac{U_A}{V_A}\left[\frac{1 - \mathrm{SGN}(U_A)\sqrt{1-4(1-F_A)}}{2}\right] \quad (12)$$

with F_A calculated from ΔU_A^{init} and SGN(U_A) is the sign of U_A.

In cases where the radial effective wake is required, correction factors following the same scheme as the tangential corrections factors above can be defined (just replacing subscript '*T*' with '*R*'). This is because the solution to the radial effective wake is also zero for a propeller alone in uniform flow.

A final remark is that for U_A values around zero the corrections are enforced to be those at the reference *J*. In the case of radial induced velocities with values close to zero in a wide region at blade mid span, U_A at *r/R=0.7* can be used for the non-dimensionalization of all correction factors.

Justifying the correction factors

A proof about the validity of the methodology can be as follows. Let us call U_A^{exact} the exact value of the axial induced velocity for an advance number J_0, and U_{A0} the approximate axial induced velocity from the potential flow method. From (3) and (4)

$$U_{A0}^{exact} = U_{A0} - \Delta U_{A0}$$

Analogously, for an advance coefficient J_1

$$U_{A1}^{exact} = U_{A1} - \Delta U_{A1}$$

Then the correction factor at J_1 can be written as

$$F_{A1} = \frac{U_{A0} + \delta U_A - \Delta U_{A0} - \delta\Delta U_A}{U_{A0} + \delta U_A} \quad (13)$$

being δU_A and $\delta\Delta U_A$ the increment in induced velocity and in correction to the induced velocity, respectively for passing from J_0 to J_1. Then

$$F_{A1} = \frac{(U_{A0} - \Delta U_{A0})\left[1 + \frac{\delta(U_A - \Delta U_A)}{U_{A0} - \Delta U_{A0}}\right]}{U_{A0}\left[1 + \frac{\delta U_A}{U_{A0}}\right]} \quad (14)$$

or

$$F_{A1} = \frac{(U_{A0} - \Delta U_{A0})\left[1 + \frac{\delta U_{A0}^{exact}}{U_{A0}^{exact}}\right]}{U_{A0}\left[1 + \frac{\delta U_A}{U_{A0}}\right]} \quad (15)$$

Usually, the corrections to the induced velocities are small compared to the induced velocities and the potential flow solution is a good approximation for the exact values. Therefore the quotient of the quantities in brackets is to the first order approximately equal to one:

$$F_{A1} \sim \frac{(U_{A0} - \Delta U_{A0})}{U_{A0}} = F_{A0}$$

A special treatment is needed when there is a location in which U_A is small. The magnitude of U_A will be not much affected by the change in advance coefficient, and therefore the correction ΔU_A could remain unchanged without altering significantly the accuracy or better can be inter/extrapolated from the neighboring points. This may happen at some control point near the hub

Alternatively, computations for two advance numbers may be used to estimate the quantities in equations (13-15), which represents a more accurate formulation of the correction factors.

Finding the correction factors

The iteration loop to find the correction factors in uniform flow is for the "exact" (a) and the "approximate" (b) approaches as follows (the steps are common to both approaches, except when marked with 'a' or 'b'),

1) Set a uniform inflow for the propeller and find the forces with the potential flow method (lifting line).

2) Express the forces of 1) in terms of body forces and introduce them in the RANS solver. Equations (1) and (2).

3) Find the total velocities at the propeller plane in the RANS solver and subtract the induced velocities obtained with the potential flow solver. A new inflow is obtained.

4a) Calculate the correction factors with equations (4) and (8) and apply the corrected induced velocities to calculate a corrected new inflow. The new inflow now is exactly the inflow at infinity.

4b) Do nothing. As the induced velocities are not corrected, the new inflow will be close but not equal to the inflow at infinity.

5) Redefine the pitch of the free vortices in the potential flow solver for each propeller with the new inflows obtained in 3).

6) Repeat step 1) through 4) with the new inflow until convergence is obtained.

7a) The correction factors are a direct output.

7b) Make an initial estimate of the correction factors with equations (4) and (8) and the final estimation using equation (12) and then (8) again.

Using the correction factors

When the effective wake is calculated using the correction factor approach, the values of the induced velocities to be subtracted from the total velocities will be $F_A\ U_A$ instead of U_A. The correction factors are determined at the control points of the lifting line, for other points on the RANS mesh the correction factors are found by interpolation.

4. IMPLEMENTATION OF THE MODEL

Propeller in open water

We choose as testing case for the procedure a propeller in uniform flow. In this particular case the effective wake is exactly known and equal to the inflow at the inlet.

The reason for this choice is that the only source of error in such simple scenario is the one due to the numerical coupling of the potential flow method with the RANS solver. Only in a scenario like this, can the coupling errors be controlled since they are isolated from other errors of different nature like those derived from using a faulty turbulent model in a ship boundary layer. In other words, we are interested here not in tackling the whole problem of effective wake prediction, but the limited problem of cancelling numerical errors due to potential flow/RANS coupling.

The reference propeller is an 8.95 m diameter, 6-bladed propeller working at an advance number of 0.71 with a thrust loading coefficient of 0.93. The number of panels used in the lifting line was 24 (more than required for engineering accuracy), and the number of cells in the radial direction in the RANS grid at the propeller plane was 25 for a coarse grid and 50 for a fine one. In the circumferential direction the number of cells was 60 and 120 for the coarse and fine grid, respectively. Figure 1 shows the fine grid at the propeller plane. The results shown next correspond to the fine grid. As the results obtained with both grids in terms of performance coefficients were very close to each other the size was considered sufficient for the demonstration of the procedure. This will be shown later in Table IV were the values of K_T, K_Q and *Eta* do not noticeably change when calculated with either the coarse or fine grid..

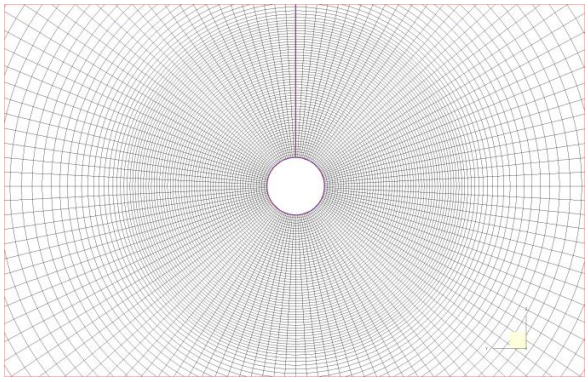

Figure 1. Computational fine grid at the propeller plane

The solution for the effective wake in this simple test is the uniform inflow velocity (V_A). Figure 2 shows the radial distribution of axial effective wake obtained at the propeller plane without correction factors. The calculated effective volumetric wake fraction ($w=1- V_E /V_A$) was $w=-0.028$ with local values at different radial stations ranging from -0.00 to +0.036. The exact one is zero. The figure shows also the corrected (and exact) effective wake, $V_E /V_A=1$, using the wake corrections.

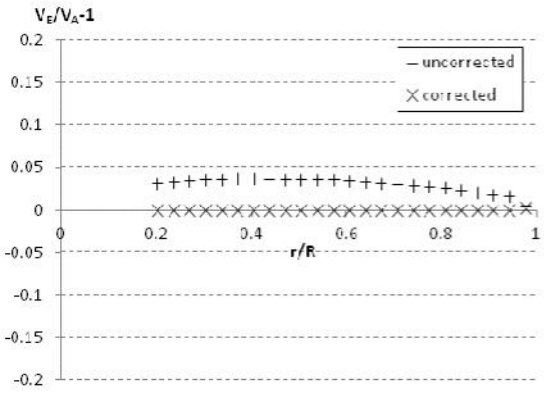

Figure 2. Radial distribution of effective wake velocities with and without corrections for the reference advance number.

Table I. Thrust coefficient for effective wake with and without corrections for the reference advance number C_T=0.98.

C_T=0.98	K_T	K_Q	η
uncorrected	0.185	0.0313	0.686
corrected & exact	0.195	0.0326	0.676
difference	5.4%	4.1%	1.5%

The thrust coefficient for the uncorrected wake is 0.185, which differs from the exact value of 0.195 in 5.4 percent. The difference in efficiency is 1.5 percent. They are shown in Table I. The thrust, torque, loading and advance coefficients are defined as usual,

$$K_T = \frac{T}{\rho n^2 D^4};\quad K_Q = \frac{Q}{\rho n^2 D^5};\quad C_T = \frac{8K_T}{\pi J^2};\quad J = \frac{V_A}{nD}$$

where T is the propeller thrust, Q is the torque, ρ is the density, n the revolutions per second and D the diameter. The propeller efficiency is η.

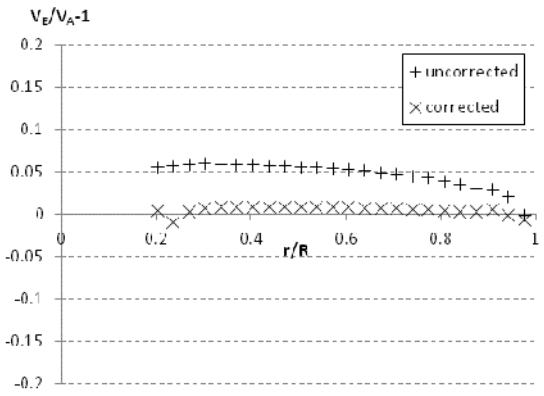

Figure 3. Radial distribution of effective wake velocities with and without correction factors at C_T=1.37. The correction factors are estimated from a calculation at C_T=0.98.

The calculations were repeated for an advance number of *J=0.655*, which increased the propeller load coefficient to C_T=1.37 (almost 50% increase). The calculation was made using the correction factors estimated at C_T=0.98, where the maximum averaged induced velocities were around 35 percent of the inflow. Table II shows a comparison of the thrust coefficients obtained with the uncorrected effective wake, and those resulting from the correction factor approach. The exact thrust coefficient is 0.231, and those estimated with the correction factor approach are 0.229 and 0.232 for the corrections calculated inside and outside the iteration loop in the RANS solver, respectively. The error in the overall thrust coefficient was less than 1 percent. For this loading the thrust coefficient calculated without corrections was 0.217, which amounted to a 6 percent error in thrust prediction.

Table II. Thrust coefficients for effective wakes with and without correction factors at C_T=1.37. Correction factors are estimated from calculation at C_T=0.98.

C_T=1.37	K_T	K_Q	η
uncorrected	0.217	0.0357	0.661
corrected 'outside'	0.232	0.0376	0.642
corrected 'inside'	0.229	0.0372	0.645
exact	0.231	0.0376	0.643

Figure 3 shows the predicted radial distribution of axial effective wake. Now maximum differences less than 1 percent at *r/R=0.4* and about 6 percent at *r/R=0.3* were found for the corrected and uncorrected case, respectively. The differences in corrected values are small in a volumetric sense as shown in Table II. The calculated volumetric wake fraction is *w=-0.0053* and *w=-0.0276* for the corrected and uncorrected case.

The number of panels in the lifting line and of cells in the viscous grid was halved and no noticeable differences (below 1 percent) were found in the estimation of the performance coefficients.

It is interesting to note that if the correction factors are calculated for C_T=1.37 and applied to the case C_T=0.98, the errors are somewhat smaller with a calculated volumetric wake fraction of *w=0.0036*. This is expected since the factors are calculated based on larger induced velocities in this case. Table III compares the thrust coefficients for this situation. Figure 4 shows the radial distribution of effective wake.

The coarse grid used in the computations yielded results similar to the fine one in performance coefficients. Table IV illustrates this fact. Even though the number of cells is 8 times smaller for the coarse grid relative to the fine one (2 times smaller in every grid direction), the differences in performance coefficients are below 1 percent for both computations with and without correction factors. This is indicative that we are in the converged range within engineering accuracy.

Finally, a test was made for an extremely demanding condition in which the propeller load was increased about 100 percent, which corresponds to an increase of C_T from 0.98 to 1.89. Table V illustrates the overall performance coefficients obtained with the correction factor approach. The differences from the exact values were about or less than 2 percent. Figure 5

shows the corresponding radial distribution of effective wake. The volumetric wake fraction was *w=-0.013*. The results in Tables III, IV and V are made with corrections factors calculated inside the iteration loop of the RANS solver.

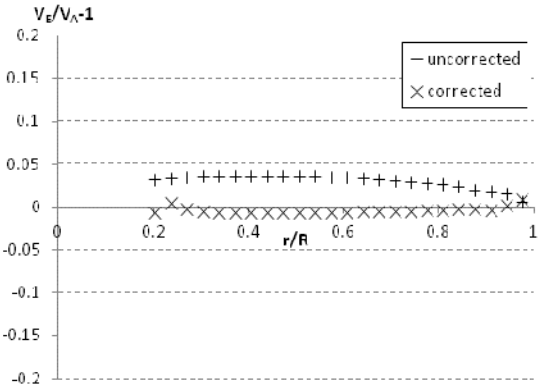

Figure 4. Radial distribution of effective wake velocities with and without correction factors at C_T=0.98. The correction factors are estimated from a calculation at C_T=1.37.

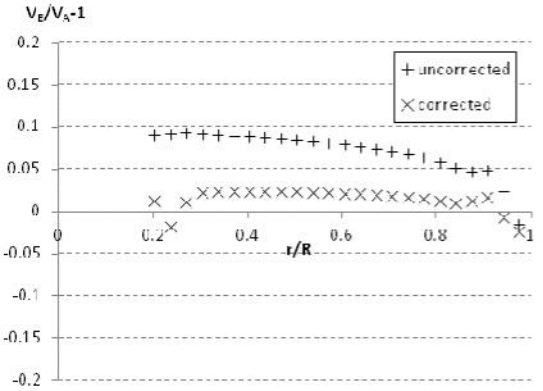

Figure 5. Radial distribution of effective wake velocities with and without correction factors at C_T=1.89. The correction factors are estimated from a calculation at C_T=0.98.

Table III. Thrust coefficients for effective wakes with and without correction factors at C_T=0.98. Correction factors are estimated from a calculation at C_T=1.37.

C_T=0.98	K_T	K_Q	η
uncorrected	0.185	0.0313	0.686
corrected	0.197	0.0329	0.674
exact	0.195	0.0326	0.676

Table IV. Thrust coefficients for effective wakes computed using the fine and coarse grids with and without correction factors at C_T=1.37. Correction factors are estimated from calculation at C_T=0.98.

C_T=1.37	K_T	K_Q	η
uncorrected-coarse	0.216	0.0355	0.663
uncorrected-fine	0.217	0.0357	0.661
corrected-coarse	0.229	0.0373	0.644
corrected-fine	0.229	0.0372	0.645

Table V. Performance coefficients for effective wakes with and without correction factors at C_T=1.89. Correction factors are estimated from calculation at C_T=0.98.

C_T=1.89	K_T	K_Q	η
uncorrected	0.247	0.0398	0.631
corrected	0.261	0.0415	0.610
exact	0.267	0.0422	0.604

5. CRP APPLICATION

In this section a CRP pod propulsion unit called RudderPod will be analyzed by actuator disks representing the fore (main) and aft (pod) propeller only from the standpoint of cancellation of numerical errors due to potential-flow/RANS model coupling. The purpose of this section is to provide some indicative values on the magnitude of such numerical errors in a particular CRP application. Comparison of computations made with and without correction factors will be indicative of how much errors due to potential flow/RANS coupling can amount in such a particular application. This requires that the correction factors are calculated at C_T close enough to the actual values so that they reproduce the exact inflow to the propeller. Flow figures are provided for illustrative purposes.

The case of study is selected from a retrofit scenario application for a container ship in which the existing single propeller was supplemented with a pod propeller working in contra-rotating mode. The housing under analysis belonged to an initial version with a non-smoothed pod geometry.

The effect of the housing on the velocities at the propeller planes is not so strong as in conventional pod units due to the fact that the CRP inflow to the strut is almost axially directed and that the strut under study is thin and streamlined. Therefore, the effective wakes at each propeller plane will be mainly caused by the effect of the other propeller. A small “potential flow” wake will be present mainly on the aft propeller plane.

The CRP unit is modeled with two actuator disks turning in opposite directions. The interactions between the actuator disks are taken into account via the bulk flow in the RANS solver, which means that the potential flow models for the two actuator disks do not interact directly with one another within the potential flow solution but solve independently the flow on each propeller. The potential-flow solution of each propeller is expressed then in terms of body forces and the body forces introduced into the RANS solution will modify in turn the input velocities to the other propeller. Therefore, there is no need of a special treatment for the CRP unit, apart from that given to the individual propellers.

The detailed steps of the procedure for the CRP case are as follows,

1) Assume an initial inflow (nominal wake) for the fore propeller and find the forces with the potential flow method (lifting line). Do the same for the aft-propeller.

2) Express the forces of 1) in terms of body forces and introduce them in the RANS solver. Do this for both propellers.

3) Calculate the induced velocities with the potential flow solver and correct them using the correction factors. Do this for both propellers.

4) Find the total velocities at the fore propeller plane in the RANS solver and subtract the corrected induced velocities obtained with the potential flow solver for the fore propeller. A new inflow is obtained. Do the same for the aft-propeller.

5) Redefine the pitch of the free vortices in the potential flow solver for each propeller with the new inflows obtained in 4).

6) Repeat step 1) through 5) with the new inflow until convergence is obtained.

It should be noted that the grid blocks representing the actuator disks in this section are those used in section 4, and for this reason the cancellation of the numerical errors due to the coupling of potential-flow/RANS methods is represented by the values shown in section 4, where both the coarse and fine grid behave similarly. This will be further illustrated in Tables IX and X where no significant differences are found between the coupling cancellation error for the CRP propellers from the coarse to the fine grid. Additionally, the corrections factors have been calculated for loadings differing from the actual ones in about 10% and 15% for the fore and aft propeller respectively, which makes the differences between calculated with corrections and exact values in uniform flow far below the 1% obtained for 50% load variation in Table II.

Table VI shows the main characteristics of the propellers. They are computed with an inflow of 9.30 m/s. The split of power between the two of them should be about 80-85 percent for the fore and 20-15 for the aft-propeller.

Figures 7 (a) and 7 (b) show the total velocities on the fore and aft-propeller disk, respectively. The two figures use the same scale in order to facilitate the comparison.

Table VI. Main particulars for the CRP unit

Main propeller		Pod propeller	
D=	8.95 m	D=	5.9 m
Z=	6	Z=	4
A_E/A_O=	0.934	A_E/A_O =	0.67
RPM=	84.18	RPM=	104

The computational mesh used a C topology around the strut and lower fin in the axial direction, and an O topology in the circumferential direction. Cylindrical blocks were added at the location of the propellers. The grids used in the present calculations consisted of 3.3 to 5.5 million cells distributed in 12 blocks. A grid sensitivity study was made before the final computations. No significant differences were found between the 5 and 5.5 million grids. The computations were made at full scale. Figure 6 shows a view of the computational mesh with the actuator disks.

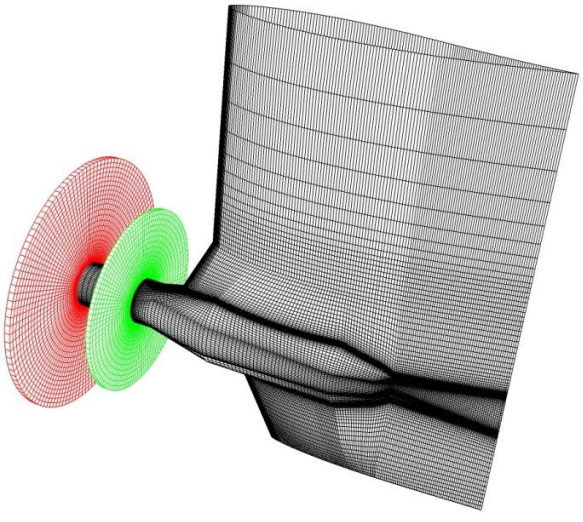

Figure 6. Computational mesh on the RudderPod unit showing the location of the actuator disks and the grid shape on the surfaces of the pod housing.

Figure 8 shows the predicted effective axial and tangential wake at the location of the fore propeller. For the axial wake, the effect of the aft-propeller on the fore one is a velocity increase limited only to the lower radii due to the small aft-propeller diameter. This increment of velocity is not large due to the low load of the aft propeller and almost cancels with the effect of the shadow of the pod housing which is stronger at the lower radii. At the outer radii a weak shadow due to the strut is visible. Also, the shear flow at the location of edge of the stream-tube caused by the aft propeller is visible.

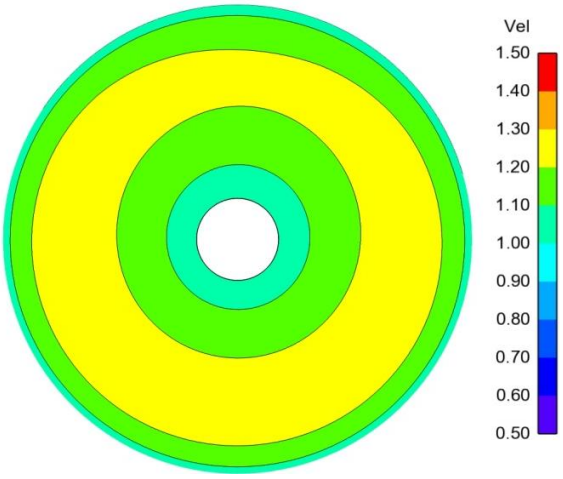

(a)

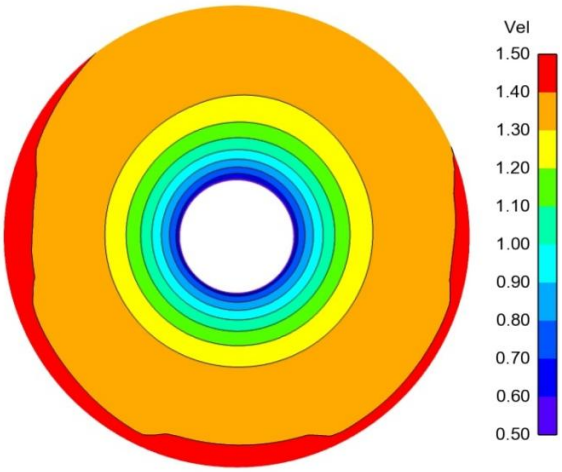

(b)

Figure 7. Total velocities at the location of the fore (a) and aft- propeller (b).

For the tangential wake, the influence of the aft propeller in the fore one is negligible for the average circumferential flow in front of a propeller, which is consistent with circulation theory predictions. The small tangential wake is mainly due to the pod.

Figure 9 shows the predicted effective axial and tangential wake at the location of the aft-propeller. The effective wakes are significantly affected by the action of the fore propeller. The lack of axial symmetry introduced by the strut is visible in the figures. Correction factors were used in the computations.

Figure 10 shows the pressures on the RudderPod surfaces. A lack of smoothing in the juncture the cylindrical part of the pod and the conical rear part is visible as a low pressure region.

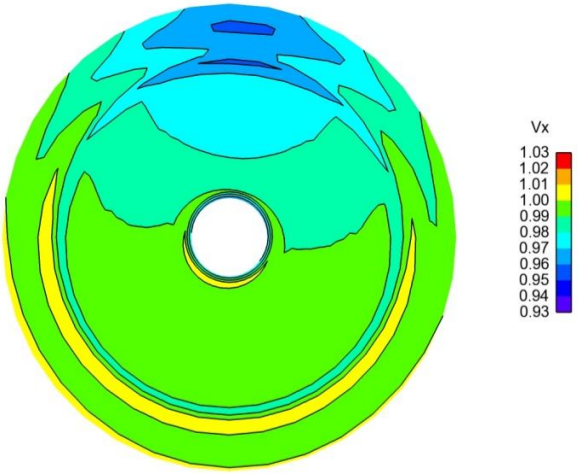

(a)

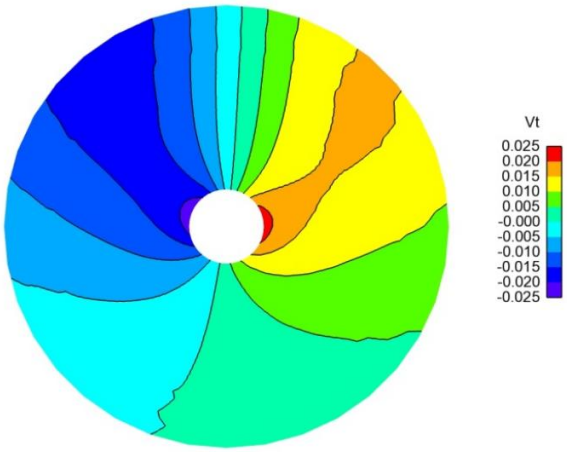

(b)

Figure 8. Axial (a) and tangential (b) effective wakes at the location of the fore propeller.

A summary of estimated forces on the propeller and pod housing is given in Tables VII and VIII for computations made with and without correction factors for the main and pod propeller, respectively.

Table VII. Effect of correction factors on the prediction of propeller performance for the main (fore) propeller in the CRP Rudderpod for the fine grid.

C_T=1.07	K_T	K_Q	η
uncorrected-fine	0.168	0.0290	0.689
corrected-fine	0.177	0.0303	0.682
difference (%)	5.4	4.5	-1.0

Table VIII. Effect of correction factors on the prediction of propeller performance for the pod (aft-) propeller in the CRP Rudderpod for the fine grid.

C_T=0.37	K_T	K_Q	η
uncorrected-fine	0.098	0.0242	0.697
corrected-fine	0.092	0.0232	0.691
difference in %	-6.1	-4.1	-1.0

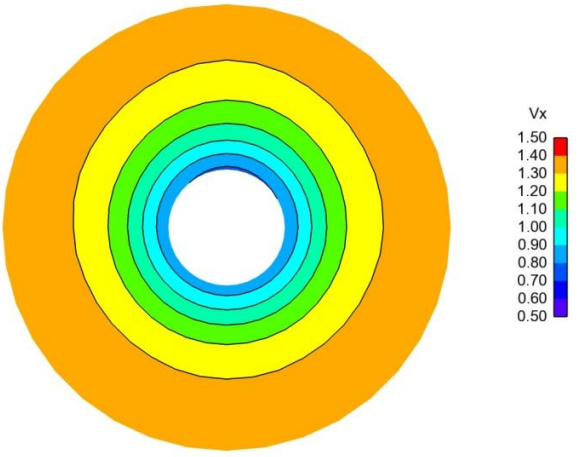

(a)

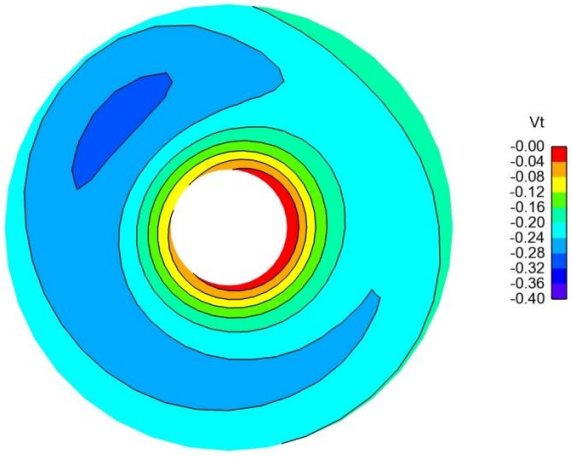

(b)

Figure 9. Axial (a) and tangential (b) effective wakes at the location of the aft-propeller.

Keeping in mind that the actual load coefficient of the propellers C_T relative to the reference load coefficient tested in uniform flow in the section 4 is less than 50%, the inflow (effective wake) to the propellers will be accurately predicted. In other words, the error in the estimation of the performance coefficients due to wrong estimation of the inflow should be far below the 1 percent difference in Table II between corrected and exact values. The Tables illustrate the magnitude of differences resulting from not using the correction factors for this particular lifting line model. For example, the thrusting force for the main (fore) propeller would be underestimated in 5.4 percent and that for the pod (aft) propeller would be overestimated in 6.4 percent. Due to the different loading in the propellers, the opposite percentages will not cancel each other in terms of total forces. The efficiency for both propellers would be overestimated in 1 percent. These differences are one of the sources of error in the general problem of calculating effective wakes.

For the aft-propeller, the changes in performance coefficients due to the correction factor approach are caused rather by the corrected inflow resulting from the fore propeller than by the corrections on the self-induced velocities since the self-induced errors are small due to the small aft-propeller loading.

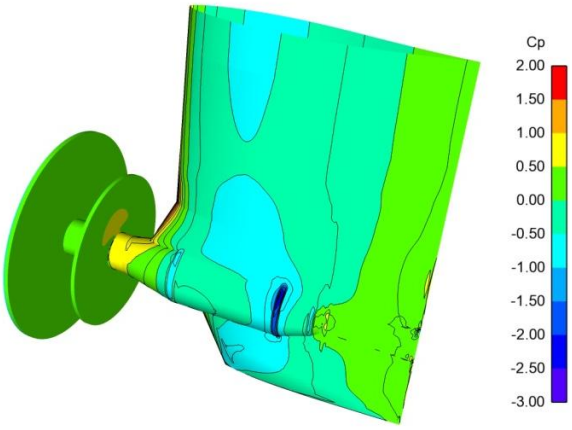

Figure 10. Pressure distribution on the Rudderpod

Tables IX and X illustrate the effect of the grid size on the corrections in performance coefficients for the fore and aft- propeller, respectively. Both the fine and the coarse grid yield similar percentages.

6. CONCLUSION

This paper presents a correction factor approach on propeller induced velocities for cancelling the numerical error due to the coupling of a potential flow

method for the simulation of the propeller with a RANS solver. By removing this error the effective wake at the propeller plane can be more accurately predicted. The propeller induced velocities approximately estimated via potential flow theory are converted into viscous induced velocities on the basis of a viscous flow RANS analysis. A lifting line method for the simulation of the propeller action was used for the demonstration of the procedure. The exact knowledge of the effective wake for a propeller in uniform flow was used as reference for quantifying the magnitude of the numerical error.

Table IX. Effect of grid size on the prediction of propeller performance for the main (fore) propeller in the CRP Rudderpod, coarse and fine grid.

C_T=1.07	K_T	K_Q	η
difference (%) fine	5.4	4.5	-1.0
difference (%) coarse	5.5	4.2	-0.9

Table X. Effect of grid size on the prediction of propeller performance for the pod (aft-) propeller in the CRP Rudderpod, coarse and fine grid.

C_T=0.37	K_T	K_Q	η
difference (%) fine	-6.4	-4.1	-1.0
difference (%) coarse	-6.1	-4.3	-1.0

The correction factors are calculated in uniform flow for one reference advance number situated in the vicinity of the region of hydrodynamic analysis and work accurately for loading changes of about +/- 50 percent. The extent to what the right effective wake is captured is a measure of the success of the correction factor approach to cancel the numerical coupling error. The procedure has been checked in uniform flow for an extreme case where the propeller loading is doubled/halved and the differences to the exact solution in force coefficients were about or less than 2 percent.

For estimating the correction factors it is recommended that the reference advance number should be a number somewhat smaller than that of the expected effective wake. The advance number for the nominal wake may be a good choice.

The correction factor approach enforces any potential flow method to give the same exact effective wake for a propeller working at the reference advance number in uniform flow. In other words, a panel method, a lifting surface method, a lifting line method, etc when supplied with corrections factors give the uniform flow at infinity as the effective wake at the propeller plane for the reference advance number. That uniform flow solution is the exact effective wake and is the same for all potential flow methods. In the paper the correction factor approach is implemented in a lifting line model.

An application to a CRP unit consisting of a main (fore) propeller and a pod (aft-) propeller has been made and coupling errors of about -5.4 and +6.4 percent were found for the thrust coefficient of the fore and aft- propeller respectively, when the correction factors are not used. The significant difference in thrust for the aft-propeller in spite of its small loading results primarily from corrections on the incoming flow and secondarily from the propeller self-induced velocities. The inflow to the aft propeller is the slipstream generated by the fore one, which is significantly altered by the effect of the correction factors.

Usually, potential-flow-based methods for the design of CRP propellers make the propeller interaction in a coupled way using as inflow for the design some effective wake common to the CRP unit. Such input effective wake does not consider differences due to the axial location of the propellers but is calculated at some axial location representative for both propellers. The present calculation decouples the effective wake of each propeller at its actual axial location and considers the interaction flow between the propellers as a part of the individual effective wakes. This makes simpler the work of the designer since an ordinary program for the design of single propellers could be used with an input effective wake which includes the interaction effects of the CRP unit.

The present procedure allows controlling one of the errors present in the calculation of effective wakes, namely the error derived from coupling a potential flow method for the representation of the propeller with a RANS solver. It can be extended to oblique flow conditions (i.e. uniform flow with a yaw angle) and to circumferentially varying body forces. This would require defining local correction factors for each panel and using several cell layers for the blades. It would be the topic of future work.

7. ACKNOWLEDGEMENTS

This work has been made within the European Union TRIPOD project under the 7th framework program (Grant # 265809). The authors wish to thank the partners in the TRIPOD consortium for their support and observations. Particularly, thanks are given to Mariano Pérez-Sobrino from UPM, Tomi Veikonheimo from ABB, Maarten Nijland from A.P. Moller – Maersk, Juan González-Adalid from SISTEMAR, Ramón Quereda and Jaime Masip from CEHIPAR and Aitor Auriarte from CintraNaval-DefCar.

REFERENCES

Choi, J.K. and Kinnas, S.A., " Prediction of Non-Axisymmetric Effective Wake by a Three-Dimensional Euler Solver," Journal of Ship Research. Vol. 45, No. 1, March 2001, pp. 13–33.

Greco, L. and Salvatore F. "Numerical Modeling of Unsteady Hydrodynamic Characteristics of a Propeller Rudder Configuration." 9th Symposium on Practical Design of Ships and Other Floating Structures (PRADS2004). Luebeck-Travemuende, Germany, 2004.

Han, Kai-Jia. "Numerical Optimization of Hull/Propeller/Rudder Configurations". Doctoral Thesis. Department of Shipping and Marine Technology, Chalmers University of Technology, Göteborg, Sweden, 2008.

Hsin, C., Chou, S., and Chen, W. "A New Propeller Design Method for the POD Propulsion System." Proc 24th Symposium on Naval Hydrodynamics, Fukuoka, Japan, (2002): 8-13.

Hoeskstra, M. "A RANS-based analysis tool for ducted propeller systems in open water condition" International Shipbuilding Progress. 53 (2006) 205–227.

Johansson, P. Davidson, L. "Modified Collocated SIMPLEC Algorithm Applied to Buoyancy-Affected Turbulent Flow Using a Multi-Grid Procedure". Numerical Heat Transfer, Part B, Vol. 28, pp. 39-57, 1995.

Kerwin, J.E., Coney, W.B. & Hsin, C.Y. 1986. "Optimum Circulation Distribution for Single and Multicomponent Propulsors." 21st ATT Conference, Washington D.C., 8 pp., 1986.

Kerwin, J., Keenan, D., Black, S., and Diggs, J. A Coupled Viscous/Potential Flow Design Method for Wake Adapted Multi-Stage, Ducted Propulsors using Generalized Geometry. Trans. SNAME, 102, 1994.

Kinnas, S.A., Jeon, C.H., Purohit, J., Tian, Y. "Prediction of the Unsteady Cavitating Performance of Ducted Propellers Subject to an Inclined Inflow," International Symposium on Marine Propulsors SMP'13, Launceston, Tasmania, May 2013.

Kinnas, S. A.,Yu, X. & Tian, Y. "Prediction of Propeller Performance under High Loading Conditions with Viscous/Inviscid Interaction and a Full Wake Alignment Model." 29th symposium on Naval Hydrodynamics, Sweden, 2012.

Kinnas, S.A., Chang,S. H., Yu, Y.H., and He, L. " A Hybrid Viscous/Potential Flow Method for the Prediction of the Performance of Podded and Ducted Propellers," Proceedings SNAME Propellers/Shafting Symposium, 2009

Kinnas, S.A., Lee, H., Gu, H., and Natarajan, S. "Prediction of Sheet Cavitation on a Rudder Subject to Propeller Flow," Journal of Ship Research. March 2007

Lee, H., Kinnas, S.A., Gu, H., and Natarajan, S. "Numerical Modeling of Rudder Sheet Cavitation Including Propeller/Rudder Interaction and the Effects of a Tunnel", Fifth International Symposium on Cavitation (CAV2003), Osaka, Japan, November 1-4, 2003.

Li. D-Q and Dyne. G (1994): "Investigation on propeller-rudder interaction by numerical methods". PhD thesis. Department of Naval Architecture and Ocean Engineering. Division of Hydrodynamics. Chalmers University of Technology. Gothenburg. Sweden.

Li, D.-Q. "Study of Propeller-Rudder Interaction Based on a Linear Method". International Shipbuilding Progress, Vol. 42, No. 431, 1995, pp. 235-257.

Lobachev, M.P., Tchitcherine, I.A., "The Full Scale Estimation for Podded Propulsion System by RANS Method." Lavrentiev Lectures, St. Petersburg (Russia), June 19-21, 2001.

Ohashi, K., and Hino, T. "Numerical Simulations of the Flows around a Ship with Podded Propulsor." Proc First International Conference on Technological Advances in Podded Propulsion, School of Marine Science and Technology, University of Newcastle, UK, (2004): 211-221.

Rijpkema, D., Starke, B., Bosschers, J. " Numerical Simulation of Propeller-Hull Interaction and Determination of the Effective Wake Field Using a Hybrid RANS-BEM Approach," International Symposium on Marine Propulsors SMP'13, Launceston, Tasmania, May 2013.

Sánchez-Caja, A., Rautaheimo, P., Salminen, E., and Siikonen, T., "Computation of the Incompressible Viscous Flow around a Tractor Thruster Using a Sliding Mesh Technique," 7th International Conference in Numerical Ship Hydrodynamics, Nantes (France), 1999.

Sanchez-Caja, A., Ory, E., Salminen, E., Pylkkänen, J.V. and Siikonen, T. “Simulation of Incompressible Viscous Flow Around a Tractor Thruster in Model and Full Scale.” The 8th International Conference on Numerical Ship Hydrodynamics September 22-25, Busan (Korea), 2003.

Sánchez-Caja, A. and Pylkkänen J.V. "Prediction of Effective Wake at Model and Full Scale Using a RANS Code with an Actuator Disk Model," 2nd International Conference on Maritime Research and Transportation, Ischia, Italy, 28-30 June, 2007.

Sánchez-Caja, A., Pylkkänen J.V. and Sipilä, T. P. ‘Simulation of the Incompressible Viscous Flow around Ducted Propellers with Rudders Using a RANSE Solver’. 27th Symposium on Naval Hydrodynamics, Korea, 2008.

Sánchez-Caja, A., Pylkkänen J.V. and Sipilä, T. P. ‘Simulation of Viscous Flow around a Ducted Propeller with Rudder Using Different RANS-Based Approaches’. First International Symposium on Marine Propulsors SMP’09, Trondheim, Norway, June 2009.

Stern, F., Kim, H.T., Zhang, D.H., Toda, Y., Kerwin, J., and Jessup, S. (1994), “Computation of Viscous Flow Around Propeller-Body Configurations: Series 60 CB = 0.6 Ship Model,” Journal of Ship Research, Vol. 38, No. 2, pp. 137-157.

Suzuki, H., Toda, Y. and Suzuki, T. "Computation of Viscous Flow around a Rudder Behind a Propeller: Laminar Flow around a Flat Plate Rudder in Propeller Slipstream". 6th International Conference on Numerical Ship Hydrodynamics, Iowa City, 2-5 August, 1993.

Zhang, D. H., Broberg, L., Larsson, L., and Dyne, G, “A Method for Computing Stern Flows with an Operating Propeller,” Royal Institution Naval Architects, 1991.